Tropical Journal of Pharmaceutical Research May 2024; 23 (5): 871-880
ISSN: 1596-5996 (print); 1596-9827 (electronic)

Available online at http://www.tjpr.org
http://dx.doi.org/10.4314/tjpr.v23i5.9

Original Research Article

Validation of UV-visible spectrophotometric method for niclosamide in different media

Hayder Yahya Mansoor Al-Jarsha, Mowafaq M Ghareeb*
Department of Pharmaceutics, College of Pharmacy, University of Baghdad, Baghdad, Iraq

For correspondence:* ***Email:* *mowafaq.abd@copharm.uobaghdad.edu.iq;* ***Tel:*** *+9647705319534*

Sent for review: 11 January 2024 *Revised accepted: 6 May 2024*

Abstract

Purpose: *To validate a UV-visible spectrophotometric technique for evaluating niclosamide (NIC) concentration in different media across various values of pH.*
Methods: *NIC was investigated using a UV-visible spectrophotometer in acidic buffer solution (ABS) of pH 1.2, deionized water (DW), and phosphate buffer solution (PBS), pH 7.4. The characterization of NIC was done with differential scanning calorimeter (DSC), powder X-ray diffraction (XRD), and Fourier transform infrared spectroscopy (FTIR). The UV analysis was validated for accuracy, precision, linearity, and robustness.*
Results: *The DSC spectra showed a single endothermic peak at 228.43 °C (corresponding to the melting point of NIC), while XRD and FTIR analysis confirmed the identity, crystallinity and purity of NIC. In all media, the measured concentration of NIC was within ± 5 % of the actual value, which confirmed accuracy. The percentage relative standard deviation values were < 1 %, reflecting the precision of the method. The range of concentration measured was between 2 and 24 µg/mL, and all coefficient of determination (R^2) values were > 0.99, indicating the linearity of the established analytical method. The limit of detection (LOD) and limit of quantification (LOQ) values were 0.122 and 0.407 µg/mL in ethanol, 0.530 and 1.766 µg/mL in ABS (pH 1.2), 0.224 and 0.747 µg/mL in DW, and 0.798 and 2.662 µg/mL in PBS, pH 7.4. The robustness was confirmed as the measured concentration under slight changes in temperatures and wavelengths were insignificant (p > 0.05).*
Conclusion: *Based on the results above, the UV-visible spectrophotometric method under investigation was validated to be accurate, precise, linear, and robust in all the different media for the determination of NIC.*

Keywords: *Niclosamide, Spectrophotometry, Validation, Accuracy, Precision, Linearity, Robustness*

Tropical Journal of Pharmaceutical Research is indexed by Science Citation Index (SciSearch), Scopus, Web of Science, Chemical Abstracts, Embase, Index Copernicus, EBSCO, African Index Medicus, JournalSeek, Journal Citation Reports/Science Edition, Directory of Open Access Journals (DOAJ), African Journal Online, Bioline International, Open-J-Gate and Pharmacy Abstracts

INTRODUCTION

Niclosamide (NIC) is an anthelmintic drug approved for infections caused by tapeworms. It is also used as a pesticide [1]. Chemically, NIC is 5-chloro-N-(2-chloro-4-nitrophenyl)-2-hydroxy-benzamide (Figure 1). It has an empirical formula of $C_{13}H_8Cl_2N_2O_4$ and a molecular weight of 327.12 g/mol.

Niclosamide (NIC) inhibits oxidative phosphorylation in the parasite by acting on the mitochondria. This leads to irreversible damage to the scolex and adjoining segments. Subsequently, the worm is separated from the wall of the intestine and expelled [1]. Recently, several pharmacological screenings have revealed that NIC is a highly promising molecule with a potential for the treatment of malignancies, bacterial infections, type II diabetes, arterial

constriction, colitis, rheumatoid arthritis, and endometriosis, as well as a wide spectrum of viral infections, including COVID-19 [3-6]. The mechanisms of action proposed for other therapeutic effects of NIC include inhibition of the transcriptional activity of signal transducers and activators of transcription 3 (STAT3) and stimulation of autophagy through signal inhibition of a mammalian target of rapamycin complex 1 (mTORC1) in MCF-7 cells expressing EGFP-LC3. The drug (NIC) has also been shown to inhibit the phosphorylation of ribosomal S6 kinases (S6K) and modulate NF-κB and the Wnt/β-catenin pathways [2].

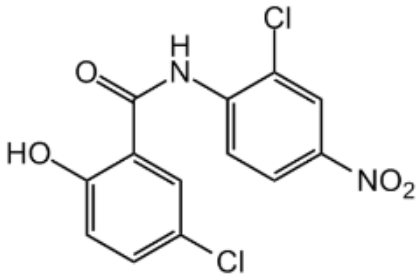

Figure 1: Chemical structure of niclosamide [2]

In cell lines, mitochondrial uncoupling induced by NIC decreased the cellular concentration of ATP and increased the ratio of ADP to ATP. Activation of AMP-activated protein kinase (AMPK) and increased lipid peroxidation have also been induced by NIC in cell lines [4]. Accordingly, NIC is an attractive molecule for future pharmaceutical research. Routinely, ethanol is employed for the UV analysis of NIC. No research has been made to analyze and validate its UV analysis using a variety of acidic, neutral, and alkaline buffers. NIC undergoes pH-dependent solubility, and research is being done to improve its solubility by altering the pH of the dosage form [3]. Therefore, there is need for a validated method for estimating its concentration not only in an organic solvent (such as ethanol) but also in acidic and basic buffer solutions. This study aimed to establish an optimized and validated spectrophotometric analytical procedure with a high level of accuracy, precision, and robustness and an adequate range of linearity for the determination of NIC concentration in various media.

EXPERIMENTAL

Materials

Niclosamide (NIC) was purchased from Hangzhou Hyper Chemicals Limited, China. Ethanol was obtained from Scharlab SL, Spain. Deionized water (DW), dibasic sodium phosphate (Na_2HPO_4), monobasic potassium phosphate (KH_2PO_4), sodium chloride (NaCl), KCl, HCl, and NaOH were purchased from Alpha Chemika, India. The analysis was performed using a UV-VIS spectrophotometer (1900i) from Shimadzu Corporation, Japan.

Characterization of NIC

Niclosamide (NIC) was characterized using the following analytical techniques:

Differential scanning calorimetry (DSC)

The melting point of NIC was determined using a differential scanning calorimeter (DSC-60 Plus) Shimadzu, Japan. A small quantity of the drug was put in an aluminum crimp pan, sealed with a crimper, and heated at a rate of 10 °C/min over a range of temperatures from 30 to 300 °C in a nitrogen gas environment. The peak temperature at which it turned into liquid was recorded as the melting point [7,8].

Powder x-ray diffraction (XRD)

XRD is used to confirm the identity and the crystallinity of materials [9]. An XRD diffractogram of NIC was obtained using a DX-2700BH diffractometer (Dandong Haoyuan Instrument, China) with a copper Kα radiation source (30 kV and 20 mA) and λ of 1.54056 Å. The range of scanning of 2-theta (2θ) was 5 – 50 degrees.

Fourier transform infrared spectroscopy (FTIR)

The FTIR spectrum of NIC between 4000 and 400 cm^{-1} was obtained via KBr disc method at room temperature using the Lambda 7600 FTIR spectrometer (USA) [10,11]. This was aimed at ascertaining the identity of NIC and the presence of any impurities in it.

Preparation of buffer solutions

The acidic buffer solution (ABS) of pH 1.2 was prepared by dissolving 2.00 g of NaCl in 1000 mL of distilled water at room temperature [12]. Then, 8.2 mL of HCl was added, and the pH was adjusted to 1.2 (if necessary) with a 1 M NaOH. Phosphate buffer solution (PBS) pH 7.4 was prepared by dissolving 8.00 g of NaCl, 0.20 g of KCl, 1.44 g of Na_2HPO_4, and 0.24 g of KH_2PO_4 in 1000 mL of DW at room temperature, followed by pH adjustment to 7.4 with HCl. The pH measurements were done using a pH meter (HI 98107) from Hanna Instruments, Inc., Italy.

Preparation of standard stock solution and corresponding dilutions

One hundred (100) mg of NIC was solubilized in about 60 mL of ethanol and then transferred to a 100-mL volumetric flask. The volume of the solution was made up to 100 mL using ethanol, resulting in a stock solution of concentration 1 µg/mL. Then, dilutions were made with either ethanol, ABS (pH 1.2), DW, or PBS (pH 7.4), to produce serial dilutions of concentration ranging from 2 to 34 µg/mL for later analytical steps. To avoid precipitation of NIC upon dilution with aqueous medium, the required volume of alcoholic stock solution was added in a drop-wise manner to the medium, with continuous stirring at 1500 rpm [3].

Determination of maximum wavelength (λ_{max})

The λ_{max} values were determined for NIC in four different media: ethanol, ABS (pH 1.2), DW, and PBS (pH 7.4). After appropriate dilutions, the absorbance was determined for each solution in triplicate between 200 and 400 nm. To comply with Beer-Lambert law, the curves of recorded λ_{maxs} were the ones in which the absorbance values were not above 1 [13].

Establishment of calibration curves

Calibration curves were established for NIC in four different media: ethanol, ABS (pH 1.2), DW, and PBS (pH 7.4). Appropriate triplicate dilutions were made to obtain different concentrations of NIC in each medium (Table 1), and their absorbance was read at their corresponding λ_{max} values.

Validation of analytical method

Accuracy

Three concentrations of NIC were prepared in triplicate for each of the four media under investigation. The concentrations were 6, 10, and 14 µg/mL. Then, the absorbance of the media was read at the corresponding wavelengths, and their concentration was calculated using the established calibration curves. The concentrations obtained were compared as percentages of their known concentration, in order to determine the level of accuracy [14].

Precision

Repeatability was determined by calculating the percent relative standard deviation (% RSD) of the triplicates used in the validation of accuracy, using Eq 1 [14,15].

$$\% \text{ RSD} = (\text{SD}/\text{mean})100 \quad \text{..... (1)}$$

Intermediate (intra-day and inter-day) precision values were determined by repeating the analysis two times every day (morning and afternoon) for three different days [14,15].

Limit of quantitation (LOQ) and limit of detection (LOD)

Values of LOD and LOQ were computed using the standard deviation (SD) of the response and the slope method, with Eq 2 and Eq 3 [16].

$$LOD = \frac{3.3 \times \sigma}{S} \quad \text{..... (2)}$$

$$LOQ = \frac{10 \times \sigma}{S} \quad \text{..... (3)}$$

where σ is the standard deviation of the response and S is the slope of the calibration curve [16].

Linearity and range

Linearity was confirmed by preparing six different concentrations of NIC in each of the four media under investigation, including one concentration below the LOQ. The analysis was done in triplicate, the curves were drawn, the linearities were assessed using the coefficient of determination of the linear regression analysis, and the ranges of linearity were recorded [14].

Robustness

By intentionally changing the experimental conditions, robustness was evaluated for each medium used at a concentration of 10 µg/mL (a value that was almost in the middle of the range for all media).

Table 1: Range and concentration used to establish calibration curve in each medium

Medium	Range (µg/mL)	Concentration (µg/mL)
Ethanol	2 – 14	2, 4, 6, 8, 10, 12, and 14
ABS (pH 1.2) DW PBS (pH 7.4)	2.4 – 24	2.4, 3.6, 7.2, 12, 16.8, 19.2, and 24

The varied factors were wavelength (± 2 nm) and temperature (samples were either refrigerated at 2 – 8 °C or put in an oven at 40 °C for 2 h before measurements) [14,17]. Analysis of variance (ANOVA) was used to determine the different levels of significance among the results.

Statistical analysis

Regression analysis was done with Microsoft® Excel® 365 MSO version 2310 Build 16.0.16924.20054) while ANOVA was performed using Minitab® statistical software version 21.2 (2022).

RESULTS

Characterization of NIC

Differential scanning calorimetry (DSC)

The thermogram in Figure 2 shows a sharp endothermic peak at 228.43 °C for NIC. This peak corresponded to and matched the reported pharmacopeial melting point of the drug at 227 – 232 °C [2].

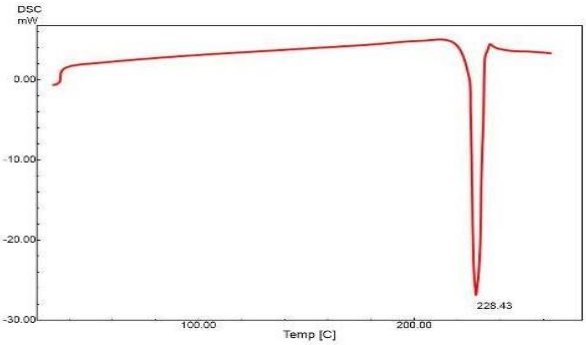

Figure 2: Differential scanning thermogram of NIC

Powder x-ray diffraction (XRD)

The diffractogram of NIC is shown in Figure 3, along with the reference diffractogram obtained from literature [18]. The NIC diffractogram showed distinguishing peaks around 2θ values of 12.6, 13.8, 19.8, 22.2, 23.4, 25.6, and 27.4.

Fourier transform infrared spectroscopy (FTIR)

Figure 4 shows the spectrum obtained for NIC which matched the previously reported spectrum in the literature [19]. The O–H stretching of the OH- group occurred as a broadband at 3244 cm^{-1}. The combination of C–O stretching and O–H in-plane deformation of hydroxyl group gave bands at 1412 and 1217 cm^{-1}. Due to the presence of an aromatic amide in NIC, it showed a stretching vibration of C=O at 1652 cm^{-1} (amide I band) and another band at 1569 cm^{-1} arising from the combined effect of C–N stretching and N–H deformation (amide II band). In addition, NIC exhibited distinctive band frequencies for benzene derivatives because of its aromatic-type structure. The most unique is the stretching of =C–H at 3101 cm^{-1} and the ring breathing vibrations in the 1600 – 1500 cm^{-1} region.

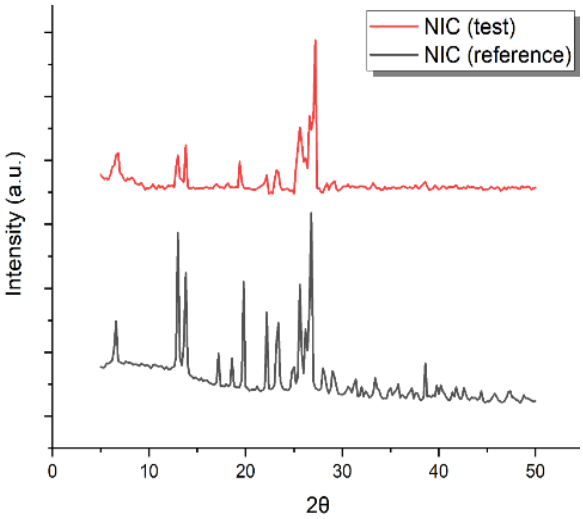

Figure 3: XRD diffractograms of reference and test NIC

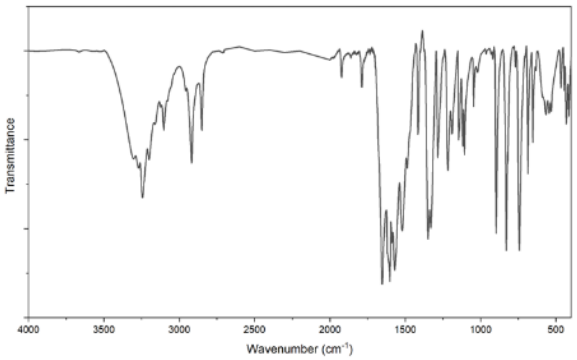

Figure 4: FTIR diagram of NIC

In addition, the substituents on the rings produced bands in the ranges of 2000 – 1650 cm^{-1} (depicting 3 bands typical for trisubstituted rings); 1600 –1450 cm^{-1}, with minor splitting of the 1500 cm^{-1} band to yield that at 1486 cm^{-1} (typical of halogenated benzenes); 1250 – 1000 cm^{-1} (as a result of the C–H in-plane deformation type), and 950 – 650 cm^{-1} (as a result of out-of-plane (wagging) deformation vibrations). Moreover, NIC displayed two intense bands at 1518 cm^{-1} and 1345 cm^{-1} representing stretching vibrations due to asymmetric and symmetric N=O, respectively [19].

Determination of maximum wavelength (λ_{max})

The spectra of NIC in ethanol, ABS (pH 1.2), DW, and PBS (pH 7.4) are shown in Figures 5A, 5B, 5C, and 5D, respectively. The value of λ_{max} in ethanol (333 nm) matches the value in the literature [3]. No literature reports are available on the λ_{max} values of NIC in ABS (pH 1.2), DW and PBS (pH 7.4).

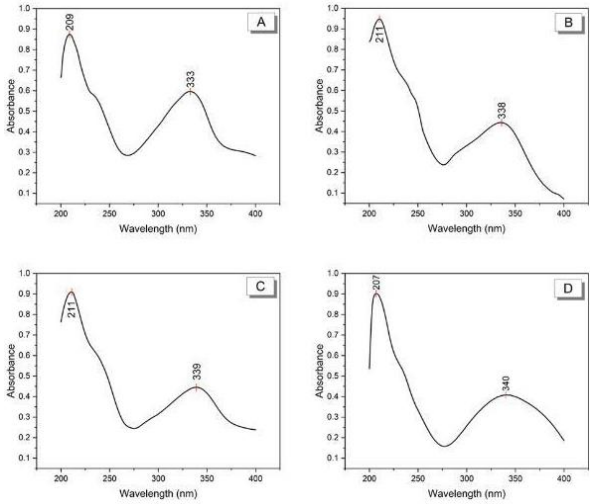

Figure 5: UV spectra of NIC in (A) ethanol, (B) ABS pH 1.2, (C) DW, and (D) PBS pH 7.4.

Calibration curves of NIC in different media

The calibration curves of NIC in the four different media are shown in Figure 6. On plotting the absorbance against concentration, straight lines were produced with $R^2 > 0.99$. This indicated that, with the concentration used, the calibration curves obeyed Beer-Lambert law [13].

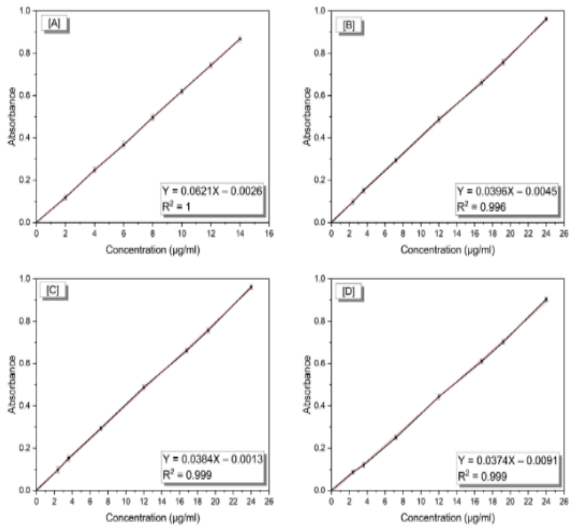

Figure 6: Calibration curves of NIC in (A) ethanol, (B) ABS pH 1.2, (C) DW, and (D) PBS pH 7.4

Validation of analytical method

Accuracy, precision, LOD and LOQ

Table 2 shows the results of the percentages obtained for accuracy and precision, in addition to LOD and LOQ (in µg/mL) for all concentrations of NIC measured in the different media.

Data for intermediate precision is shown in Table 3. All RSD values were below 5 %, reflecting both high levels of precision and insignificance between groups. Accordingly, the intermediate precision of the method was confirmed.

Linearity and range

Figure 7 shows the linearity curves obtained, R^2 values, and their ranges for NIC in the different media used.

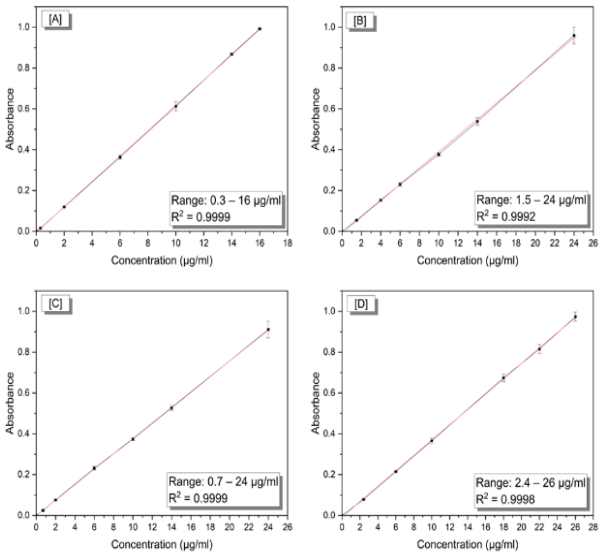

Figure 7: Linearity curves and ranges of NIC in (A) ethanol, (B) ABS pH 1.2, (C) DW, and (D) PBS pH 7.4

Robustness

The values obtained for the concentration of NIC under investigation for robustness (10 µg/mL) at different wavelengths and temperatures for different media are displayed in Table 4.

DISCUSSION

In pharmaceutical analysis, DSC is a method used to evaluate the thermal characteristics of medicinal compounds, such as melting point and polymorphic transitions. It provides essential information for drug development and quality control through the evaluation of medication stability and purity.

Table 2: Accuracy, precision, LOD, and LOQ for NIC in different media

Medium	Actual concentration (µg/ml)	Mean concentration measured (µg/mL)	SD	Error (%)	Accuracy (%)	Precision (%RSD)	LOD (µg/mL)	LOQ (µg/mL)
Ethanol	6	6.10	0.032	1.61	101.6	0.53	0.122	0.407
	10	9.98	0.041	-0.17	99.8	0.41		
	14	13.91	0.016	-0.67	99.3	0.12		
ABS pH 1.2	6	5.89	0.053	-1.87	98.1	0.89	0.530	1.766
	10	10.15	0.053	1.47	101.5	0.52		
	14	14.18	0.067	1.28	101.3	0.47		
DW	6	5.85	0.054	-2.50	97.5	0.93	0.224	0.747
	10	10.05	0.080	0.51	100.5	0.79		
	14	14.31	0.054	2.24	102.2	0.38		
PBS pH 7.4	6	5.83	0.027	-2.81	97.2	0.46	0.798	2.662
	10	9.94	0.041	-0.60	99.4	0.41		
	14	13.91	0.027	-0.67	99.3	0.19		

Table 3: Intermediate precision data for NIC in different media

Solvent	AC (µg/ml)	Day 1 morning			Day 1 afternoon			Day 2 morning			Day 2 afternoon			Day 3 morning			Day 3 afternoon		
		CM (µg/mL)	SD	P (% RSD)	CM (µg/ml)	SD	P (% RSD)	CM (µg/ml)	SD	P (% RSD)	CM (µg/ml)	SD	P (% RSD)	CM (µg/ml)	SD	P (% RSD)	CM (µg/ml)	SD	P (% RSD)
Ethanol	6	6.10	0.032	0.53	6.02	0.033	0.55	5.96	0.03	0.54	6.04	0.032	0.53	5.95	0.032	0.53	5.99	0.033	0.55
	10	9.98	0.041	0.41	9.79	0.039	0.40	10.17	0.04	0.41	10.11	0.039	0.39	9.86	0.040	0.41	9.85	0.041	0.42
	14	13.91	0.016	0.12	13.72	0.016	0.12	14.01	0.02	0.11	14.09	0.016	0.11	14.24	0.016	0.12	14.11	0.016	0.11
ABS pH 1.2	6	5.89	0.053	0.89	5.81	0.052	0.90	5.92	0.05	0.89	5.92	0.051	0.87	6.03	0.054	0.90	5.97	0.052	0.86
	10	10.15	0.053	0.52	10.12	0.052	0.51	9.95	0.05	0.53	9.96	0.053	0.53	9.84	0.052	0.53	10.13	0.053	0.52
	14	14.18	0.067	0.47	14.27	0.067	0.47	14.06	0.07	0.48	13.94	0.067	0.48	14.01	0.069	0.49	13.73	0.068	0.50
DW	6	5.85	0.054	0.93	5.92	0.054	0.91	5.96	0.06	0.93	6.11	0.054	0.88	6.01	0.053	0.89	6.01	0.053	0.88
	10	10.05	0.080	0.79	10.24	0.079	0.77	10.03	0.08	0.80	9.91	0.082	0.82	9.85	0.080	0.81	10.04	0.079	0.78
	14	14.31	0.054	0.38	14.21	0.054	0.38	13.75	0.06	0.40	13.88	0.055	0.39	13.92	0.053	0.38	14.01	0.055	0.39
PBS pH 7.4	6	5.83	0.027	0.46	5.91	0.027	0.46	6.09	0.03	0.45	6.08	0.026	0.43	6.07	0.027	0.44	5.88	0.027	0.47
	10	9.94	0.041	0.41	9.83	0.040	0.41	9.93	0.04	0.41	9.84	0.041	0.42	10.05	0.041	0.41	10.01	0.040	0.40
	14	13.91	0.027	0.19	13.79	0.027	0.20	13.97	0.03	0.20	14.18	0.027	0.19	14.19	0.027	0.19	13.89	0.027	0.19

Note: CM; Mean concentration measured; AC: Actual prepared concentration, P: Precision, RSD: Relative standard deviation

Table 4: Robustness data for NIC at different wavelengths and temperatures for different media

Medium	λ_{max} or Temp range	Mean concentration measured (mcg/ml)				SD	P-value
		Replicate 1	Replicate 2	Replicate 3	Average		
Ethanol	333 nm	9.86	10.04	10.09	10.00	0.12	
	331 nm	9.95	10.07	10.12	10.05	0.09	0.413
	335 nm	9.85	10.06	9.85	9.92	0.12	
	Room (25 – 30 °C)	9.88	10.06	10.11	10.02	0.12	
	Refrigerator (2 – 8 °C)	9.83	10.03	10.01	9.96	0.11	0.582
	Oven (40 °C)	9.80	9.98	9.98	9.92	0.10	
ABS pH 1.2	333 nm	10.01	10.11	9.86	10.00	0.13	
	331 nm	10.09	10.14	9.91	10.05	0.12	0.61
	335 nm	9.96	10.06	9.79	9.94	0.14	
	Room (25 - 30)	9.99	10.06	9.89	9.98	0.09	
	Refrigerator (2 - 8)	9.96	9.99	9.81	9.92	0.10	0.4
	Oven (40)	9.91	9.94	9.73	9.86	0.11	
DW	333 nm	10.03	10.16	9.85	10.02	0.16	
	331 nm	10.09	10.22	9.88	10.06	0.17	0.803
	335 nm	9.98	10.11	9.83	9.97	0.14	
	Room (25 - 30)	10.09	10.19	9.90	10.06	0.14	
	Refrigerator (2 - 8)	10.06	10.14	9.77	9.99	0.19	0.706
	Oven (40)	9.98	10.11	9.70	9.93	0.21	
PBS pH 7.4	333 nm	10.00	9.90	10.08	9.99	0.09	
	331 nm	10.06	10.00	10.35	10.14	0.19	0.225
	335 nm	9.92	9.82	10.03	9.92	0.11	
	Room (25 - 30)	10.03	9.98	10.11	10.04	0.07	
	Refrigerator (2 - 8)	9.92	9.90	10.06	9.96	0.09	0.424
	Oven (40)	9.87	9.82	10.08	9.92	0.14	

The sharp peak of NIC obtained, and the absence of other extrinsic peaks indicate its high degree of purity and crystallinity [7].

The technique of XRD is an essential method for determining if a drug molecule is crystalline or amorphous. This allows for assessment of the purity, stability, and general quality by providing comprehensive information on the molecular and structural properties of the compound. Furthermore, XRD plays a crucial role in monitoring the structural changes that medications may undergo in response to different environmental factors [20]. The peaks are consistent with data from the literature, thereby confirming the crystallinity and purity of the NIC sample used [18,20].

The λ_{max} of a drug may vary owing to solvatochromism, which is a phenomenon where the interactions between the drug and the solvent affect the electronic structure of the drug, resulting in shifts in the wavelength of maximum absorption. For NIC, upon increasing the pH across aqueous media from ABS (pH 1.2), distilled water, and PBS (pH 7.4), there were noticeable increases in λ_{max}. This can be attributed to the increased solubility of NIC at higher pH levels due to deprotonation and ionization of its phenolic group. As a result, electronic transitions require more energy in the form of longer wavelengths. Therefore, when NIC was exposed to higher pH values, its solubility and capacity to form ions increased, causing a shift towards longer wavelengths (redshift) in the λ_{max}. This shift indicates a change in the electronic state of the molecule in response to variations in pH [21].

Needham [3] reported the calibration curve of NIC. However, the reported absorbance was below 0.5. The study did not utilize concentration with high absorbance, and two sources of NIC were used in the research. Therefore, heterogeneous results were obtained. The correlation between concentration and absorbance, as described in the Beer-Lambert equation, is demonstrated by the resultant calibration curve. The obtained R^2 value (> 0.99) indicated a strong linear relationship between absorbance and concentration, confirming that absorbance consistently changed in accordance with the assumption of linearity for absorbance below 1 in the Beer-Lambert law [3,19]. Accordingly, the calibration curves obtained enabled measurement of the NIC concentration based on its absorbance within this range.

Accuracy, in analytical terms, refers to the degree to which a measurement corresponds to the true value of the quantity being measured. A margin of error of 5 % is often seen as acceptable in analytical methods, serving as evidence of the method's precision. The accuracy of the UV analytical method was validated by confirming that the percentage of

error across measured concentration was within a range of ± 5 % of the actual concentration. The precision refers to the ability of the analytical method to consistently provide findings that are close to each other, with a low %RSD indicating the method's reliability. The precision and intermediate precision values of the UV analytical method of NIC (assessed by the values of %RSD) were ± 1 and 5 %, respectively. Accordingly, the precision is verified for the method [22].

Linearity in analytical techniques indicates that the assay results exhibit a direct and proportionate relationship with analyte concentration in the sample within a given range. When validating linearity, it is recommended to use a minimum of five datum points covering the whole range, along with an extra point below LOQ, in order to build a thorough calibration curve [14]. For NIC, the linear regression analysis produced calibration curves that showed a linear correlation across all the tested media (R^2 > 0.999). This comprehensive method demonstrates the linearity of the UV analytical technique for NIC, which validates its use for this important analytical parameter.

Robustness refers to the capacity of the method to withstand changes in experimental circumstances while still retaining reliability and consistency [14]. The robustness of the UV spectrophotometric analysis of NIC was assessed by deliberately altering the temperature and λ max under controlled conditions [23]. The lack of statistical significance in the results despite applying these changes confirms the robustness of the method. Therefore, this illustrates the analytical potential of the procedure to generate reliable and consistent results, even when exposed to slight operational variations, thereby confirming its suitability for routine analysis.

CONCLUSION

Validation of the UV-visible spectrophotometric analysis for niclosamide in different media across several pH values is accurate, precise, linear, and robust. Since NIC is a promising molecule with several potential indications, this method would be useful in future research.

DECLARATIONS

Acknowledgements

None.

Funding

This research did not receive any specific grant

from funding agencies in the public, commercial, or not-for-profit sectors.

Ethical approval

None provided.

Availability of data and materials

The datasets used and/or analyzed during the current study are available from the corresponding author on reasonable request.

Conflict of Interest

No conflict of interest associated with this work.

Contribution of Authors

We certify that the work in question was performed by the author(s) identified in this article. All claims referring to claims related to the material in this paper will have to be borne by the writers.

Use of Artificial Intelligence

Artificial intelligence was not employed in the conduct of this research.

REFERENCES

1. *Bayer AG. Yomesan® (Niclosamide) PIL. 2022; (cited 2024 Jan 3). Available from: https://www.bayer.com/sites/default/files/YOMESAN_EN_PI.pdf.*
2. *Kapale SS, Chaudhari HK. Niclosamide and challenges in chemical modifications: A broad review on enhancement of solubility. J Indian Chem Soc 2021; 98(12): 100262.*

3. Needham D. The pH dependence of niclosamide solubility, dissolution, and morphology: Motivation for potentially universal mucin-penetrating nasal and throat Sprays for COVID-19, its variants and other viral infections. Pharm Res 2022; 39(1): 115-141.
4. Chen W, Mook RAJ, Premont RT, Wang J. Niclosamide: Beyond an antihelminthic drug. Cell Signal 2018; 41: 89-96.
5. Manna MJ, Abu-raghif A, Muhsin HY. The effect of niclosamide in acetic acid-induced colitis: An experimental study. Prensa Méd Argent 2019; 105(5): 309-316.
6. Abdulamir AS, Gorial FI, Saadi SJ, Maulood MF, Hashim HA, Alnuaimi AS, Abdulrrazaq MK. A randomized controlled trial of effectiveness and safety of niclosamide as add-on therapy to the standard of care measures in COVID-19 management. Ann Med Surg (Lond) 2021; 69: 102779.
7. Nawar MT, Alaa AA. Formulation and evaluation of montelukast sodium nanoparticles for transdermal delivery. Int J Drug Deliv Technol 2021; 11(2): 530-538.
8. Mina SA, Nawal AR, Yehia IK. Preparation and characterization of time-controlled drug delivery system of sumatriptan using natural polymers. Iraqi J Pharm Sci 2018; 27(1): 89-99.
9. Rusel ZF, Shahlaa EE. Preparing nanosilica particles from rice husk using precipitation method. Baghdad Sci J 18(3): 2021; 494-500.
10. Segall A. Preformulation: The use of FTIR in compatibility studies. J Innov Appl Pharm Sci 2019; 4(3): 1-6.
11. Redha IA, Mohammed RA, Luma SA. Synthesis of new quinoline -2-one derivatives. Iraqi J Sci 2015; 56(3): 2468-2480.
12. Suresh K, Matzger AJ. Enhanced drug delivery by dissolution of amorphous drug encapsulated in a water-unstable metal-organic framework (MOF). Angew Chem Int Ed Engl 2019; 58(47): 16790-16794.
13. Al-Sabbagh B, Abdulrazzaq NN. Measuring dye concentration using a low-cost visible-light spectrophotometer. Iraqi J Chem Pet Eng 2022; 23(2): 27-33.
14. ICH. Guidance for industry: Q2(R1) Validation of analytical procedures: Text and method. ICH Harmonized Tripartite Guideline 2021.
15. Danzer K, Statistical evaluation of analytical results, in Analytical Chemistry: Theoretical and metrological fundamentals, K Danzer, Editor. Springer Berlin Heidelberg: Berlin, Heidelberg 2007; 65-100 p.
16. Al-Abachi M, Abed S, Al-Uzri W. Spectrophotometric determination of chloramphenicol in pharmaceutical preparations. Irq Nat J Chem 2014; 55: 231-242.
17. Yaseen A, Ghareeb MM, Alsaffar D, Ming T, Gazzali A. Development and validation of HPLC method for the detection of fusidic acid loaded in non-ionic and cationic nanoemulsion-based gels. Biomed Pharmacol J 2023; 16(1): 573-580.
18. Guo LQ, Xu KL, Ma XL, Li SS, Li H. X-ray powder diffraction data for niclosamide, C13H8N2O4Cl2. Powder Diffr 2015; 30(4): 375-377.
19. Bhavana V, Chavan RB, Mannava MKC, Nangia A, Shastri NR. Quantification of niclosamide polymorphic forms – A comparative study by Raman, NIR and MIR using chemometric techniques. Talanta 2019; 199: 679-688.
20. Naveen K, Thakral RL, Zanon RC, Kelly ST. Applications of powder X-ray diffraction in small molecule pharmaceuticals: Achievements and aspirations. J Pharm Sci 2018; 107(12): 2969-2982.
21. Anderson RJ, Bendell DJ, Groundwater PW. Organic spectroscopic analysis. United Kingdom: Royal Society of Chemistry 2004.
22. Kumari B, Khansili A. Analytical method development and validation of UV-visible spectrophotometric method for the estimation of vildagliptin in gastric medium. Drug Res 2020; 70(9): 417-423.
23. Rahman H, Haque SM. Development and validation of chromatographic and spectrophotometric methods for the quantitation of rufinamide in pharmaceutical preparations. Turk J Pharm Sci 2022; 19(3): 267-272.